EFFECT OF LIQUID WATER CONTENT ON BLADE ICING SHAPE OF HORIZONTAL AXIS WIND TURBINE BY NUMERICAL SIMULATION

by

Yan LI[a*], Ce SUN[a], Yu JIANG[a], Xian YI[b], and Yingwei ZHANG[a]

[a] Heilongjiang Provincial Key Laboratory of Technology and Equipment for the Utilization of Agricultural Renewable Resources in Cold Region, Northeast Agricultural University, Harbin, China
[b] State Key Laboratory of Aerodynamics, China Aerodynamics Research and Development Center, Mianyang, China

Original scientific paper
https://doi.org/10.2298/TSCI180627234L

To research the law of the icing accretes on near the tip part of rotating blade of large-scale horizontal axis wind turbine (HAWT) influenced by liquid water content (LWC), the icing distribution on a HAWT rotor with rated power of 1.5 MW was simulated based on a Quasi-3D computation method. About 30% part length of blade from tip along span wise to blade root which are the most serious icing area was selected to research. Eight sections of this 30% part were decided and the ice distribution on each sections were simulated. Five kinds of LWC from 0.2 g/m^3 to 1.4 g/m^3 and two kinds of temperatures including –6 °C and –18 °C were selected. The medium volume droplet is 30 mm. Three kinds of icing time were selected to analyze the effects of icing time on ice accretion. The icing shape evaluate method was applied to quantitatively analyze the icing shape obtained under different conditions. The results show that the icing shapes are all horn icing shape under the different LWC when the temperature is –6 °C. The icing shapes change from horn icing shape to streamline icing shape with LWC increasing under the temperature of –18 °C. The icing accretes on blade surface layer by layer with icing time increasing. The closer the section blade tip, the more icing accretes. This study can be as reference for the research on anti-icing and de-icing technologies for large-scale HAWT.

Key words: *horizontal axis wind turbine, icing, numerical simulation, liquid water content, icing shape*

Introduction

In order to solve the energy crisis and mitigate global warming, many countries pay attention green and renewable energy conservation [1-3]. Wind energy as a green and revewable energy has been developmented in recent years [4]. The HAWT as the main type of wind turbine has been constructed at all over the world [5]. To obtatin more wind energy, many wind turbines were installed in the cold area [6]. However, the cold climate has a greatly effect on the performance of wind turbine when the icing accretes on blade surface [7]. The icing accretes on balde surface will change its aerodynamic characteristics and load distribution, which will decreases the output power and affects the reliability and safety of wind turbine [8]. Therefore, the icing problems on wind turbine are getting more and more attention. To research the characteristics of icing on

* Corresponding author, e-mail: liyanneau@163.com

blade surface, there are two main kinds of method including icing wind tunnel test and numerical simulation. With the rapidly development of CFD, the numerical simulation has been widely used in research the law of icing accretes on blade surface [9]. In 1953, messigner researched the rule of heat and mass transfer model of icing distribution on blade surface and this model was called messinger model which is the foundemental model for icing simulation method [10]. Many simulation softwares and codes had been developed such as LEWICE, LEWICE3D, ONERA, *etc.* [11-13]. However, these softwares and codes are serving for aircraft icing, rarely codes can be developed to research the icing on rotating blade. Based on previous research, a Quiasi-3D numerical simulation method was developed to investigate the icing distribution on blade surface in previous research [14]. The icing distribution on blade surface will be quickly calculated by this Quiasi-3D numerical simulation [15]. The accuracy of this method has been verified by comparing the calculate results with other codes and icing tunnel test.

In the previous research, the icing distribution on blade surface of a 1.5 MW HAWT has been simulated. The results show that the serious icing area of blade is located at the part from blade tip to 30% length. Therefore, this research mainly calculated the icing distribution on this area. Eight kinds of sections and five kinds of LWC from 0.2 g/m^3 to 1.4 g/m^3 were selected to simulate under two kinds of temperatures. The medium volume droplet (MVD) is 30 mm. The results show that the icing shapes are all horn icing shape under different LWC when the temperature is –6 °C. The icing shapes change from streamling icing shape to horn icing shape with LWC increasing when the temperature is –18 °C. The icing area, stationary point thickness and icing volume increasing with LWC increases. The most icing are is 1303226 mm^2, the most stationary point thickness is 438 mm and the most icing volume is 418417595 mm^3. This research could provide the data base for de-anti icing system.

Geometric model and method

Wind turbine model

Figure 1 shows the rotor diagram of the HAWT which was selected to simulated in this study. It's rated power is 1.5 MW at the wind speed of 11 m/s. The rotor diameter, D, is 83 m and the blade length, L, is 39.2 m. The blade is made by glass fiber reinforced plastic. Based on the previous researches, the icing almost occurs at the part between tip and 70% blade length from tip to root. The most serious icing area between blade tip to root of 30% blade length was selected to simulate in this research. Eight Sections of this area decided to calculated. Figure 2 shows the diagram of local velocities at airfoil. The U_∞ is the wind speed, where V is the tangential velocity and $V = r\omega$, where W is the resultant velocity. To make the simulation simplifying, the resultant velocity, W, is turned into horizontal location by using a rotation angle, ψ. This operation is based on the assumption that there is no water flowing along blade span under rotational condition. Although this may lead to some errors comparing with the actual condition, the simplification is effective for evaluating the overall

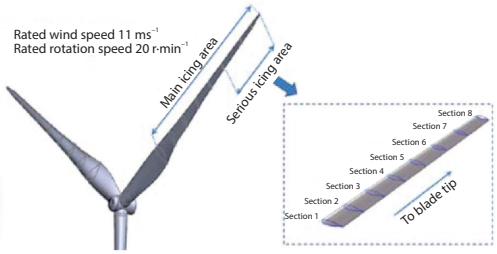

Figure 1. Diagram of rotor model for simulation

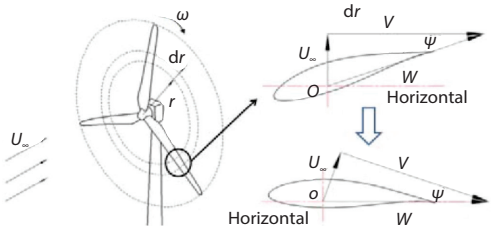

Figure 2. Local velocities at blade airfoil

icing characteristics on blade. Therefore, a 3-D rotating model is simplified into a 2-D model. We named the method as Quasi-3-D computational method**.** The main working parameters of each airfoil are shown in tab. 1.

Table 1. Working parameters of each blade section

Section	r [m]	c [m]	U_∞ [ms^{-1}]	V [ms^{-1}]	W [ms^{-1}]	ψ [°]	Re
S_1	29.18	1.28	11	60.11	61.1	10.4	5354018
S_2	30.68	1.21	11	63.20	64.2	9.9	5318008
S_3	32.18	1.14	11	66.29	67.2	9.4	5244484
S_4	33.68	1.06	11	69.38	70.3	9.1	5101405
S_5	35.18	0.99	11	72.47	73.3	8.6	4967842
S_6	36.68	0.91	11	75.56	76.4	8.3	4759522
S_7	38.18	0.84	11	78.65	79.5	7.9	4571672
S_8	39.68	0.76	11	81.74	82.5	7.6	4292360

Simulation method

The air-flow field is low-velocity viscous flow which can be calculated by N-S equation and solved by the SIMPLE method. The N-S equation is:

$$\frac{\partial \rho\phi}{\partial t} + \nabla(\rho\vec{\mathrm{v}}\phi - \Gamma_\phi \mathrm{grad}\phi) = q_\phi \tag{1}$$

where r is the air density, ϕ – the transport variable, $\vec{\mathrm{v}}$ – the air velocity, Γ_ϕ – the air temperature, and q_ϕ – the source item.

The air has not compressed in the calculation process, so the mass conservation equation is:

$$\frac{\partial \rho}{\partial t} + \nabla(\rho\,\vec{\mathrm{v}}) = 0 \tag{2}$$

If the turbulence model used in this paper is k-ε model, the turbulent kinetic energy equation is:

$$\frac{\partial(\rho k)}{\partial t} + \frac{\partial(\rho\varepsilon u_i)}{\partial x_i} = \frac{\partial}{\partial x_j}\left[\alpha_k \mu_{eff}\frac{\partial \varepsilon}{\partial x_j}\right] + G_k + \rho\varepsilon \tag{3}$$

The turbulent energy dissipation rate equation is:

$$\frac{\partial(\rho\varepsilon)}{\partial t} + \frac{\partial(\rho\varepsilon u_i)}{\partial x_i} = \frac{\partial}{\partial x_j}\left[\alpha_\varepsilon \mu_{eff}\frac{\partial \varepsilon}{\partial x_j}\right] + \frac{C_{1\varepsilon}\varepsilon}{K}G_k - C_{2\varepsilon}\rho\frac{\varepsilon^2}{k} \tag{4}$$

The impingement limit was calculated by the Lagrangian method and solved based on Runge-Kutta method. The initial time-step used in the trajectory integration is 10^{-5} seconds. The Lagrangian equation is given:

$$M_d\frac{\mathrm{d}^2\vec{x}_d}{\mathrm{d}t^2} = (\rho_d - \rho_a)V_d\vec{\mathrm{g}} + \frac{1}{2}C_d A_d \rho_a\left|\vec{\mathrm{u}}_a - \vec{\mathrm{u}}_d\right|(\vec{\mathrm{u}}_a - \vec{\mathrm{u}}_d) \tag{5}$$

where ρ_d is the density of droplets, ρ_a – the density of air, $\vec{\mathrm{g}}$ – the acceleration of gravity, A_d – the area of water droplet facing wind, V_d – the volume of water droplet, C_d – the drag coefficient, $\vec{\mathrm{u}}_a$ – the local wind velocity, and $\vec{\mathrm{u}}_d$ – the water droplet velocity.

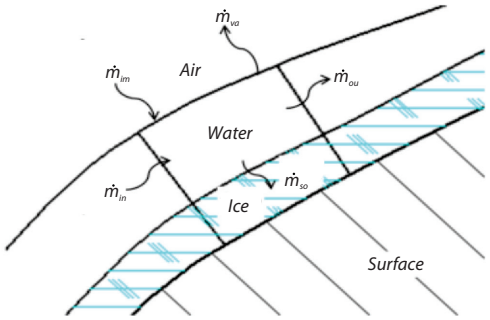

Figure 3. Mass conservation in single control body

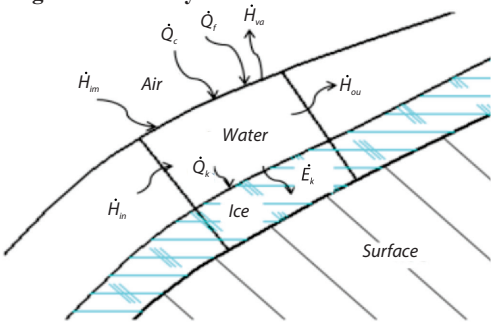

Figure 4. Energy conservation in single control body

Based on the control body theory, the process of icing which droplets impact on blade is solved by mass and energy conservation equations. The mass and energy conservation on the surface of the single control body are shown in figs. 3 and 4, respectively.

According to the mass conservation, the weight of current control body equals to the difference between mass of water going into the surface of control body and the leaving ones. The equation is:

$$m'_{in} + m'_{im} - m'_{va} - m'_{ou} = m'_{so} \tag{6}$$

The eq. (1) is usually given:

$$m'_{ou} = (1-f)(m'_{im} + m'_{in}) - m'_{va} \tag{7}$$

where m_{in} is mass of water flow from upstream into control body, m_{im} – the super-cooled droplets impacting on the blade, m_{va} – the mass of water transforming into steam by evaporation or sublimation, m_{ou} – the mass of water droplets which is not freezes and flow into downstream, m_{so} – the mass of water which was changed to ice, and f – the icing ratio.

The surface energy of the control body is subdivided into eight items. According to the first law of thermodynamics, the energy balance equation:

$$\dot{E}_{so} + \dot{H}_{va} + \dot{H}_{ou} - \dot{H}_{in} - \dot{H}_{im} = \dot{Q}_f - \dot{Q}_c - \dot{Q}_k \tag{8}$$

where $\dot{E}_{so}$ is the energy of water during freezing, $\dot{H}_{va}$ – the heat of evaporation of water droplets or ice surface, $\dot{H}_{ou}$ – the energy of droplets out the body, $\dot{H}_{in}$ – the energy of droplets into the body, $\dot{H}_{im}$ – the impact kinetic energy into the water heat flux, $\dot{Q}_{\text{tf}}$ – the energy of air friction heating, $\dot{Q}_c$ – the convective hot flow of wall and the environment, and $\dot{Q}_k$ – the heat between ice and water.

Meshing

Figure 5 shows the main information about computational domain and meshing around the airfoil. To accurately calculate the flow field changing around the surface of airfoil, the grids around the airfoil encrypted and represented. To research the optimum grid number to calculate, the grid independence verification tests had been carried. Figure 6 shows the relationship between the lift coefficient with grid number. Considering the computing power of computer and the accuracy of the grid, the grid number was set more than 36000 under per simulations in this study.

Table 2 shows the material properties of water and ice. Table 3 shows the main environmental parameters including temperature, LWC, MVD, and icing time which were decided to research the ice accretion on blade surface with the increasing of time.

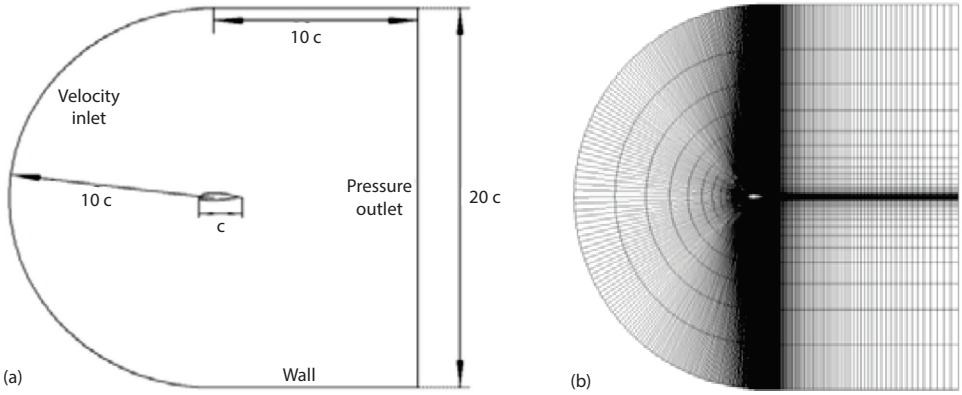

Figure 5. Mesh around blade airfoil

Table 2. Material properties of water and ice

Material	ρ [gm^{-3}]	μ [Pa · s]	q [Jkg^{-1}]	c [J/kg°C]
Water	1000	$1.7921 \cdot 10^{-3}$	$2.48 \cdot 10^{6}$	4200
Ice	800	–	$3.35 \cdot 10^{5}$	2100

Table 3. Environmental parameters for simulation

Temperature [°C]	LWC [gm^{-3}]	MVD [μm]	t [s]
–6 –18	0.2 0.4 0.6 1.0 1.4	30	1800 3600 5400

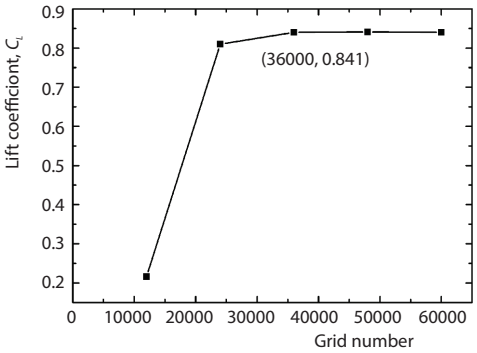

Figure 6. Meshing independence verification

Results and discussion

Icing shape and distribution

Figure 7 shows the icing shapes of Section 2, 4, 6, and 8 under different LWC at the icing time of 5400 seconds under the temperature is –18 °C. It can be found that the streamline icing shape occurs at the LWC between 0.2-0.4 g/m^3, and horn icing shape occurs at the LWC between 0.6-1.4 g/m^3. Under the smaller LWC conditions of 0.2-0.4 g/m^3, when the droplets impact on the blade surface, the droplets will change to ice immidiately. Under the higher LWC conditions of 0.6-1.4 g/m^3, the droplets change to water film and spread from middle to two sides due to the effect of flow wind. The reason is the higher the LWC, the lower the total heat transfer efficiency. The icing shape changes bigger and bigger with LWC increasing under certain section when the other parameters are the same.

Main parameters of icing shape

Definition of main parameters of 2-D icing shape

In this research, the evaluate method proposed by Yan was applied to quantitatively anlyze the icing shapes obtained under different conditions [15]. The parameters used to evaluate 2-D icing shape on airfoil are shown in figs. 8 and 9.

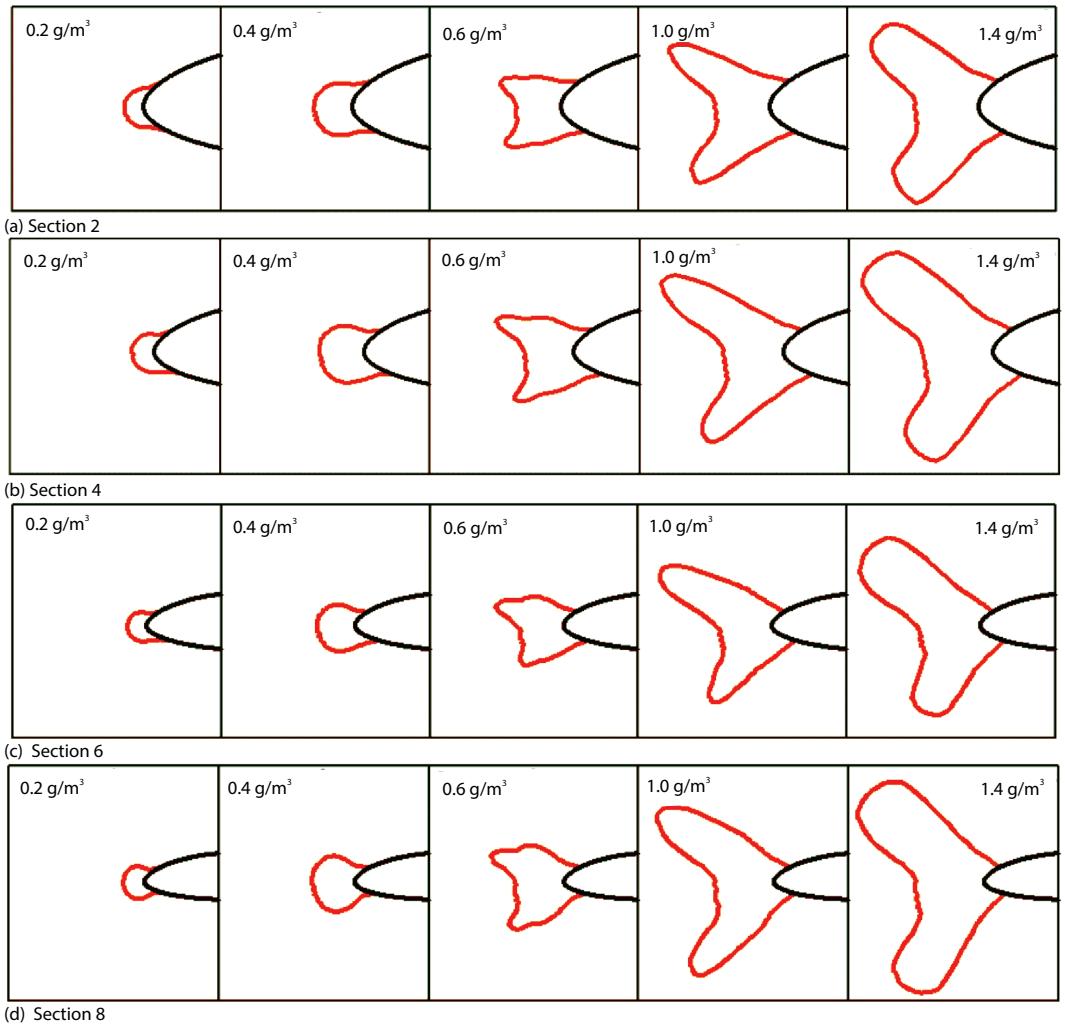

Figure 7. Icing shapes of different sections at different LWC and icing time of 5400 seconds under the temperature is –18 °C; (a) Section 2, (b) Section 4, (c) Section 6, and (d) Section 8

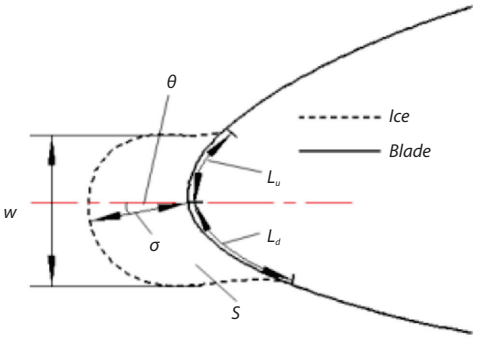

Figure 8. Typical characteristics of streamlined shape ice

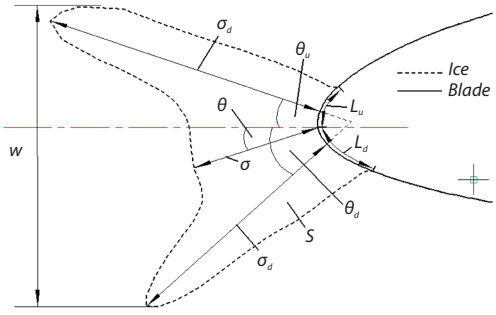

Figure 9. Typical characteristics of horn shape ice

In this research, the icing area, the maximum stagnation thickness and icing volume were selected to quantitatively analyze the characteristics of icing distribution.

The maximum thickness of streamlined icing shape is:

$$\sigma_{\max} = \sigma \tag{9}$$

The maximum thickness of horn icing shape is:

$$\sigma_{\max} = \max[\sigma, \sigma_u, \sigma_d] \tag{10}$$

These three kinds of parameters are dimensionless due to the shapes and sizes of icing on different airfoils along wingspan are different. The dimensionless parameters are shown:

The dimensionless maximum icing area $\sigma_{\max}$ is:

$$\eta_\sigma = \frac{\sigma}{c} \tag{11}$$

The dimensionless maximum thickness of icing η_S is:

$$\eta_S = \frac{S}{S_b} \tag{12}$$

The dimensionless icing volume of icing η_V is:

$$\eta_V = \frac{V_i}{V_b} \tag{13}$$

where σ is the stationary point thickness, c – the chord length of airfoil, S – the icing area, S_b – the surface area of blade, V_i – the volume of icing, and V_b – the volume of blade.

Analysis of dimensionless parameters of icing shape

Figure 10 shows the relationship between dimensionless icing area and LWC on different blade sections at the time of 5400 seconds. The icing area increases with the LWC increasing. Closer the section the blade tip, bigger the icing area is. The biggest icing area reaches 200% of airfoil area, and the maximum icing area is 1303226 mm^2 of the Section 8 under the LWC is 1.4 g/m^3 and the temperature is –18 °C. Figure 11 shows the relationship between dimensionless maximum stationary thickness and LWC on different blade sections at the time of 5400 seconds. The The maximum stationary thickness is 438 mm of the Section 8 at the temperature of –18 °C under the LWC is 1.4 g/m^3, which is about 57% of the airfoil chord length. Figure 12 shows the the

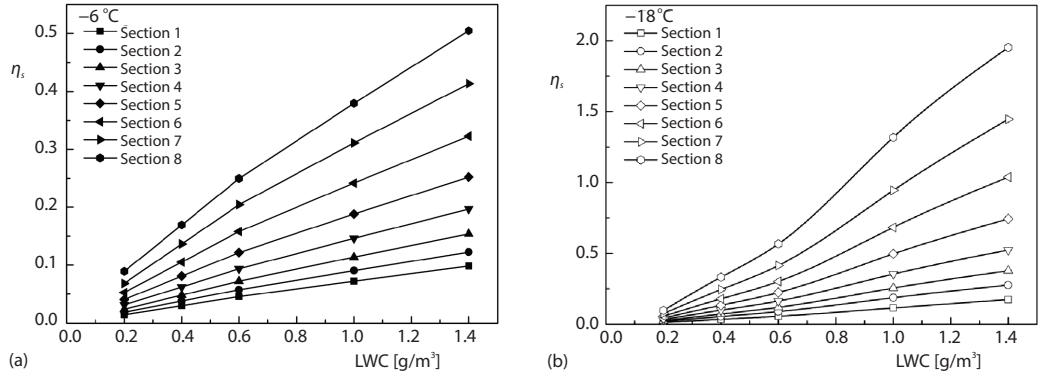

Figure 10. The relationship between dimensionless icing area and LWC of different blade sections at time of 5400 seconds under different temperatures; (a) T = –6 °C, (b) T = –18 °C

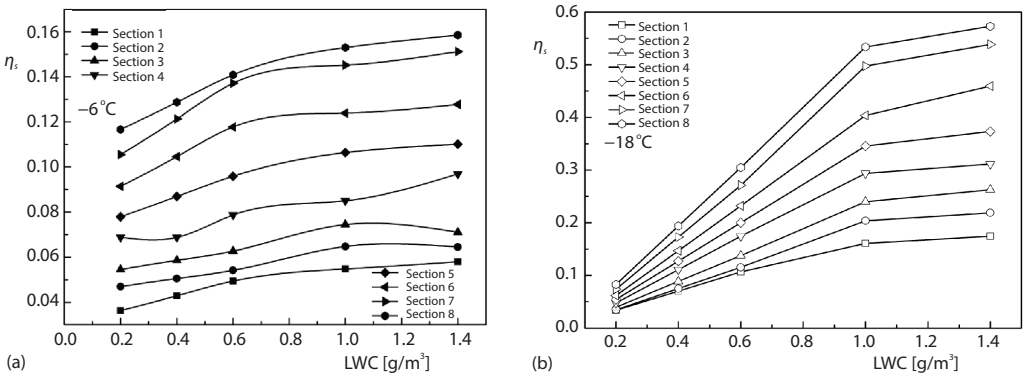

Figure 11. The relationship between maximum dimensionless stationary point thickness and LWC of different blade sections at time of 5400 seconds under different; (a) T = –6 ºC, (b) T = –18 ºC

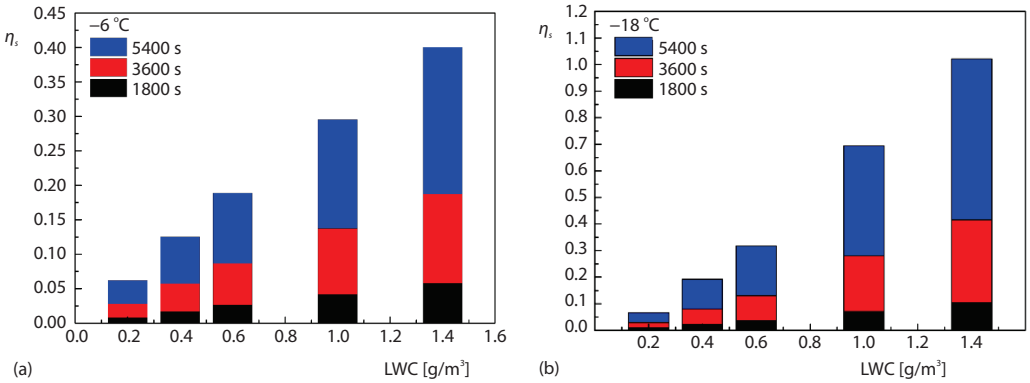

Figure 12. The relationship between dimensionless icing volume of blade and different LWC at different time; (a) T = –6 ºC, (b) T = –18 ºC

relationship between dimensionless icing volume of blade and different temperatures at different time. The icing volume increases with LWC increasing generally. The biggest icing volume is 418417595 mm^3, which is about 60% of the blade volume

Conclusion

In this work, the icing distribution on a HAWT rotor with rated power of 1.5 MW was simulated based on a Quasi-3D computation method to study the law of the icing accretes on near the tip part of rotating blade of the HAWT influenced by LWC. Two kinds of icing shapes including streamling icing shape and horn icing shape were obtained under different LWC. Under the temperature of –6 °C, the icing shapes are all horn icing shape under different LWC. Under the temperature of –18 °C, the icing shapes change from streamline icing shape to horn icing shape with the LWC increasing. At certain LWC, the icing shapes of different sections along the turbine blade are different. Closer the section the blade tip, bigger the icing shape is. At certain blade section, the icing accretes layer by layer on airfoil surface and keeps the similar icing shape with the time increasing under different LWC researched in this study. The icing area, stationary point thickness and icing volume increase with the LWC increasing under the other parameters are the same. The The maximum icing area is about 200% of the airfoil area and the maximum stationary point is about 57% of the airfoil length. The icing volume is about 60% of blade volume.

Acknowledgment

This research was sponsored by the projects supported by National Natural Science Foundation of China (NSFC, No. 51576037). The authors would like to thank to their supports.

Nomenclature

L – icing limit, [mm]
LWC – liquid water content, [gm^{-3}]
MVD – medium volume droplet diameter, [μm]
m' – mass, [g]
Q – quantity of heat, [J]
S – icing area, [mm^2]
T – icing time, [s]
U_∞ – velocity of wind flows, [ms^{-1}]
V – peripheral speed, [ms^{-1}]
W – resultant velocity, [ms^{-1}]
w – icing width, [mm]

Greek symbols

η – dimensionless method, [–]
θ – deflection angle of icing, [–]
σ – icing thickness, [mm]
ψ – rotation angle of airfoil, [º]

References

[1] Zhang, Y., *et al.,* Wind Energy Rejection in China: Current Status, Reasons and Perspectives, *Renewable and Sustainable Energy Rev*iews, *66* (2016), Dec., pp. 322-344
[2] Zhao, Z., *et al.* Enhancement Approaches of Aerodynamic Performance of Lift-Type Vertical Axis Wind Turbine Considering Small Angle of Attack (in Chinese), *Journal of Drainage and Irrigation Machinery Engineering, 36* (2018), 2, pp. 146-153
[3] Yan ,L., *et al.* Starting Performance Effect of a Truncated-Cone-Shaped Wind Gathering Device on Small-Scale Straight-Bladed Vertical Axis Wind Turbine, *Energy Conversion and Management, 167* (2018), July, pp. 70-80
[4] Zhang, Y., *et al.* A Review of Methods for Vortex Identification in Hydroturbines, *Renewable and Sustainable Energy Reviews, 81* (2018), Part 1, pp. 1269-1285
[5] Yan L., *et al.* An Icing Wind Tunnel Test on Icing Character Istics of Cylinder Roating Arounde a Shaft (in Chinese), *Acta Aeronautica et Astronautica Sinica, 38* (2017), 2, pp. 116-126
[6] Yan, L., *et al.* Scaling Method of the Rotating Blade of a Wind Turbine for a Rime Ice Wind Tunnel Test, *Energies*, *12* (2019), 4, pp. 626-627
[7] Sarah, K. B., *et al.* The Impact of Ice Formation on Wind Turbine Performance and Aerodynamics, *Journal of Solar Energy Engineering, 133* (2011), 1, pp. 311-328
[8] Yan, L., Kotaro T., Fang F., *et al.* A Wind Tunnel Experimental Study of Icing on Wind Turbine Blade Airfoil, *Energy Conversion and Management, 85* (2014), Sept., pp. 591-595
[9] Xian, Y., Numerical Computation of Aircraft Icing and Study on Icing Test Scaling Law (in Chinese), Ph. D. thesis, China Aerodynamics Research and Development Center Graduate School, Mianyang, China, 2007
[10] Mssinger, B. L., Equilibrium Temperature of an Unheated Icing Surface as a Function of Air Speed, *Journal of the Aeronautical Sciences, 20* (1953), 1, pp. 29-42
[11] Ruff, G. A., Berkowitz, B. M., Users Manual for the NASA Lewis Ice Accretion Prediction Code (LEWICE), NASA CR185129, USA, 1990
[12] Wright, W. B., Users Manual for the Improved NASA Lewis Ice Accretion Code LEWICE 1.6. NASA CR198355, 1995
[13] Hedde, T., Guffond D., Development of a 3-D Icing Code Comparison with 3-D Experimental Shapes, AIAA-92-0041, 1992
[14] Yan, L., *et al.,* Icing Distribution of Rotating Blade of Horizontal Axis Wind Turbine Based on Quasi-3D Numerical Simulation, *Thermal Science, 22* (2018), 2, pp. 1191-1201
[15] Yan, L., *et al.* Temperature Effect on Icing Distribution near Blade Tip of Large-Scale HAWT by Numerical Simulation, *Advances in Mechanical Engineering, 10* (2018), 11, pp. 1-13

Paper submitted: June 27, 2018
Paper revised: December 2, 2018
Paper accepted: February 1, 2019